Available online at www.sciencedirect.com
SCIENCE DIRECT
Thermochimica Acta 446 (2006) 101–105
thermochimica acta
www.elsevier.com/locate/tca

# Synthesis, structural characterization and thermochemical reactivity of tris(ethylenediamine)zinc tetracyanozincate, a precursor for nanoscale ZnO

Yanzhi Guo, Rainer Weiss, Roland Boese, Matthias Epple *

*Institute of Inorganic Chemistry, University of Duisburg-Essen, Universitaetsstrasse 5-7, D-45117 Essen, Germany*

Available online 9 February 2006

Dedicated to Prof. Wolfgang F. Hemminger on the occasion of his 65th birthday.

**Abstract**

The binuclear complex tris(ethylenediamine)zinc tetracyanozincate was prepared and characterized by single-crystal X-ray structure analysis. It consists of distorted $[Zn(en)_3]^{2+}$ octahedra and $[Zn(CN)_4]^{2-}$ tetrahedra. The thermolysis under air was studied by thermogravimetry, and the resulting product (ZnO) was characterized by X-ray diffraction and scanning electron microscopy, showing compact particles with a diameter of 100–300 nm.


*Keywords:* Zinc oxide; Coordination compounds; Crystal structure; Thermolysis; Scanning electron microscopy

## 1. Introduction

Zinc oxide nanostructures have been the subject of intense interest due to their potential wide-ranging applications [1,2]. Zinc oxide is a wide band gap semiconductor which is used, e.g., in electronics, photoelectrochemistry, and sensor technology [3–5]. In catalysis, a mixed catalyst containing copper and zinc oxide is used in methanol synthesis. Recent studies indicate that the Cu–ZnO interface plays an important role under reducing reaction conditions [6]. Nanostructured ZnO with various morphologies such as nanorods, nanowires, nanotubes, nanosheets and nanodiscs were prepared by different synthetic methods [7–12]. Vapour phase growth at high temperature is the major physical method to prepare ZnO nanostructures [13]. The wet-chemistry synthesis is generally carried out with solutions of zinc salts in water or alcohols, to which hydroxide is added which leads to the precipitation of ZnO [14]. The preparation of ZnO nanostructures by thermolysis of organometallic [15] or molecular precursors [16] was also reported.

Metal oxides can be obtained by thermolysis of metal cyanide coordination compounds under mild conditions [17–21]. In the work presented here, zinc oxide was prepared by thermolysis of $[Zn(en)_3][Zn(CN)_4]$, a new binuclear complex that decomposes to zinc oxide at moderate temperature under oxidizing conditions. This process was followed by thermogravimetry and the product was characterized with respect to its crystallinity and morphology. It was of interest whether the loss of the ligands would lead to a fine particulate ZnO phase which might be of interest, e.g., for heterogeneous catalysis. The neutral ligand ethylenediamine should be a good leaving group as well as the cyanide which may be released as cyanogen, $(CN)_2$ or undergo oxidative combustion [20].

## 2. Materials and methods

Single-crystal structure analysis was carried out with a Siemens SMART CCD area detector system and for calculations (solution and refinement) the program package Bruker AXS SHELXTL Version 6.12 was used.

Thermogravimetry was carried out with a Netzsch STA 409 TG-DTA apparatus. Samples were heated from room temperature to 1000 °C at a rate of $5\,K\,min^{-1}$ under dynamic $O_2$ atmosphere at a flow rate of $50\,mL\,min^{-1}$.

IR characterization of the products was performed with a Bruker Vertex 70 instrument in KBr pellets. High-resolution

* Corresponding author. Fax: +49 201 183 2621.
*E-mail address:* matthias.epple@uni-due.de (M. Epple).

0040-6031/$ – see front matter © 2006 Elsevier B.V. All rights reserved.
doi:10.1016/j.tca.2006.01.002

X-ray powder diffractometry was carried out in transmission geometry at beamline B2 at HASYLAB/DESY, Hamburg, Germany, with a wavelength of $\lambda = 0.71$ Å. Scanning electron microscopy was carried out with a Leo 420 instrument on gold-sputtered samples.

## 3. Results and discussion

The binuclear coordination compound was prepared by coordinating $Zn^{2+}$ (zinc nitrate) with ethylenediamine, giving a cationic complex, and by coordinating $Zn^{2+}$ (zinc nitrate) with cyanide (KCN), giving an anionic complex, respectively. Mixing of both solutions in equal amounts led to a white precipitate of the title compound. The final concentration of zinc was 20 mmol in 50 mL of water, used in stoichiometric amounts according to Eqs. (1)–(3). All reactions were carried out in water at room temperature in high yield. Single crystals were isolated from the precipitate:

$$Zn^{2+} + 3en \rightarrow [Zn(en)_3]^{2+} \quad (1)$$

$$Zn^{2+} + 4CN^- \rightarrow [Zn(CN)_4]^{2-} \quad (2)$$

$$[Zn(en)_3]^{2+} + [Zn(CN)_4]^{2-} \rightarrow [Zn(en)_3][Zn(CN)_4] \downarrow$$
$$(en = H_2N–CH_2–CH_2–NH_2) \quad (3)$$

Elemental analysis gave 29.74% Zn (calculated: 31.50%), 28.14% C (calculated: 28.93%), 5.37% H (calculated: 5.83%), and 32.39% N (calculated: 33.74%). Zn was determined by atomic absorption spectroscopy, and carbon, hydrogen and nitrogen by combustion analysis.

The structural elements of this coordination compound are shown in Fig. 1. At the cationic zinc site (Zn1), zinc is octahedrally coordinated by three bidentate ethylenediamine ligands, and on the anionic site (Zn11), it is tetrahedrally coordinated by four monodentate cyanide ligands. The octahedron around Zn1 is distorted as it has been reported earlier for $[Zn(en)_3]^{2+}$-complexes [22–25]. The tetrahedral $[Zn(CN)_4]^{2-}$ unit is also distorted. The proximity of the cyanide ligand (N13) to one of the hydrogen atoms of ethylendiamine at N2 (2.291 Å) seems to

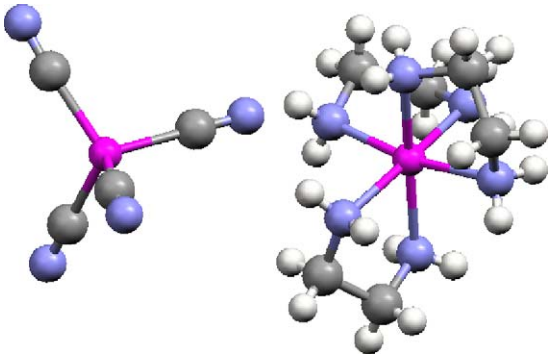

Fig. 1. The two structural elements, $[Zn(en)_3]^{2+}$ (central atom: Zn1) and $[Zn(CN)_4]^{2-}$ (central atom: Zn11), of the crystal structure of tris(ethylene diamine) zinc tetracyanozincate. Zinc: magenta; carbon: grey; nitrogen: blue; hydrogen: white.

Table 1
Crystallographic data of tris(ethylenediamine)zinc tetracyanozincate

| Crystal structure data | |
|---|---|
| Calculated formula | $Zn_2C_{10}H_{24}N_{10}$ |
| Calculated density | 1.525 g cm$^{-3}$ |
| Wavelength | 0.71073 Å |
| Space group | $P2_1/n$ |
| Crystal system | Monoclinic |
| $a$ | 10.7073 Å |
| $b$ | 15.2124 Å |
| $c$ | 11.1041 Å |
| $\beta$ | 91.967° |
| $Z$ | 4 |
| Unit cell volume | 1807.61 Å$^3$ |
| Independent reflections | 4514 [$R$(int) = 0.0187] |
| $R$ indices [$I > 2\sigma(I)$] | $R_1 = 0.0158$<br>$wR_2 = 0.0426$ |
| $R$ indices (all data) | $R_1 = 0.0186$<br>$wR_2 = 0.0444$ |

Atomic coordinates

| Atom | $x$ | $y$ | $z$ | $U$ (eq) |
|---|---|---|---|---|
| Zn1 | 8027 | 1704 | 2671 | 23 |
| N1 | 7277 | 352 | 2676 | 29 |
| C1 | 6076 | 360 | 3283 | 37 |
| N2 | 6160 | 1955 | 3308 | 29 |
| C2 | 5370 | 1195 | 2978 | 39 |
| N3 | 7488 | 1918 | 768 | 29 |
| C3 | 8635 | 1936 | 66 | 31 |
| N4 | 9770 | 1368 | 1838 | 27 |
| C4 | 9542 | 1242 | 536 | 31 |
| N5 | 8626 | 3074 | 2948 | 34 |
| C5 | 9534 | 3093 | 3981 | 39 |
| N6 | 8883 | 1610 | 4498 | 31 |
| C6 | 9065 | 2509 | 4971 | 41 |
| Zn11 | 2825 | 4706 | 2272 | 27 |
| C11 | 2226 | 5063 | 3905 | 36 |
| N11 | 1919 | 5184 | 4865 | 56 |
| C12 | 2924 | 5693 | 1048 | 33 |
| N12 | 3064 | 6231 | 357 | 52 |
| N13 | 5578 | 3909 | 2519 | 38 |
| C13 | 4595 | 4201 | 2434 | 29 |
| N14 | 1096 | 3179 | 1221 | 46 |
| C14 | 1702 | 3735 | 1601 | 32 |

Atomic coordinates ($\times 10^4$) and equivalent isotropic displacement parameters (Å$^2 \times 10^3$) are given. $U$ (eq) is defined as one-third of the trace of the orthogonalized $U_{ij}$ tensor.

be responsible for the elongated bond between zinc (Zn11) and this cyanide ligand (C13–N13). The shortest Zn–Zn distances in the structure are 5.380 and 5.552 Å. The main crystallographic data are comprised in Tables 1 and 2.

The infrared spectrum of the zinc complex is shown in Fig. 2. All expected IR bands are visible: 3359/3365/3294 cm$^{-1}$ ($NH_2$ valence), 2956/2893 cm$^{-1}$ ($CH_2$ valence), 2144 cm$^{-1}$ (C≡N valence), 1589 cm$^{-1}$ (N–H deformation), 1467 cm$^{-1}$ (C–H deformation), 1328/1278 cm$^{-1}$ (C–H), and 1045/1001/959 cm$^{-1}$ (C–C valence).

The thermolysis of $[Zn(en)_3][Zn(CN)_4]$ under oxygen occurs in a multi-step process (Fig. 3). First, probably a part of

Table 2
Bond lengths and bond angles of tris(ethylenediamine)zinc tetracyanozincate

| Bond lengths | |
|---|---|
| Zn(1)–N(4) Å | 2.1723(9) |
| Zn(1)–N(2) Å | 2.1774(9) |
| Zn(1)–N(3) Å | 2.1960(10) |
| Zn(1)–N(5) Å | 2.1994(10) |
| Zn(1)–N(6) Å | 2.2025(10) |
| Zn(1)–N(1) Å | 2.2079(9) |
| N(1)–C(1) Å | 1.4729(15) |
| C(1)–C(2) Å | 1.5113(18) |
| N(2)–C(2) Å | 1.4716(15) |
| N(3)–C(3) Å | 1.4770(15) |
| C(3)–C(4) Å | 1.5149(16) |
| N(4)–C(4) Å | 1.4704(14) |
| N(5)–C(5) Å | 1.4780(18) |
| C(5)–C(6) Å | 1.5127(19) |
| N(6)–C(6) Å | 1.4752(16) |
| Zn(11)–C(11) Å | 2.0194(13) |
| Zn(11)–C(12) Å | 2.0302(12) |
| Zn(11)–C(14) Å | 2.0306(12) |
| Zn(11)–C(13) Å | 2.0473(12) |
| C(11)–N(11) Å | 1.1404(18) |
| C(12)–N(12) Å | 1.1350(17) |
| N(13)–C(13) Å | 1.1427(15) |
| N(14)–C(14) Å | 1.1374(16) |
| **Bond angles** | |
| N(4)–Zn(1)–N(2) | 172.58(4)° |
| N(4)–Zn(1)–N(3) | 80.01(3)° |
| N(2)–Zn(1)–N(3) | 94.18(4)° |
| N(4)–Zn(1)–N(5) | 91.81(4)° |
| N(2)–Zn(1)–N(5) | 93.15(4)° |
| N(3)–Zn(1)–N(5) | 93.42(4)° |
| N(4)–Zn(1)–N(6) | 92.30(4)° |
| N(2)–Zn(1)–N(6) | 94.01(4)° |
| N(3)–Zn(1)–N(6) | 169.64(4)° |
| N(5)–Zn(1)–N(6) | 79.80(4)° |
| N(4)–Zn(1)–N(1) | 95.71(4)° |
| N(2)–Zn(1)–N(1) | 79.92(4)° |
| N(3)–Zn(1)–N(1) | 93.28(4)° |
| N(5)–Zn(1)–N(1) | 170.69(4)° |
| N(6)–Zn(1)–N(1) | 94.40(4)° |
| C(1)–N(1)–Zn(1) | 108.47(7)° |
| N(1)–C(1)–C(2) | 110.02(10)° |
| C(2)–N(2)–Zn(1) | 107.90(7)° |
| N(2)–C(2)–C(1) | 109.03(10)° |
| C(3)–N(3)–Zn(1) | 108.30(7)° |
| N(3)–C(3)–C(4) | 109.93(9)° |
| C(4)–N(4)–Zn(1) | 109.46(7)° |
| N(4)–C(4)–C(3) | 109.28(9)° |
| C(5)–N(5)–Zn(1) | 107.90(8)° |
| N(5)–C(5)–C(6) | 109.08(10)° |
| C(6)–N(6)–Zn(1) | 108.22(8)° |
| N(6)–C(6)–C(5) | 109.21(10)° |
| C(11)–Zn(11)–C(12) | 115.34(5)° |
| C(11)–Zn(11)–C(14) | 108.81(5)° |
| C(12)–Zn(11)–C(14) | 109.67(5)° |
| C(11)–Zn(11)–C(13) | 110.09(5)° |
| C(12)–Zn(11)–C(13) | 105.50(5)° |
| C(14)–Zn(11)–C(13) | 107.11(5)° |
| N(11)–C(11)–Zn(11) | 173.32(12)° |
| N(12)–C(12)–Zn(11) | 175.31(11)° |
| N(13)–C(13)–Zn(11) | 179.16(11)° |
| N(14)–C(14)–Zn(11) | 178.39(12)° |

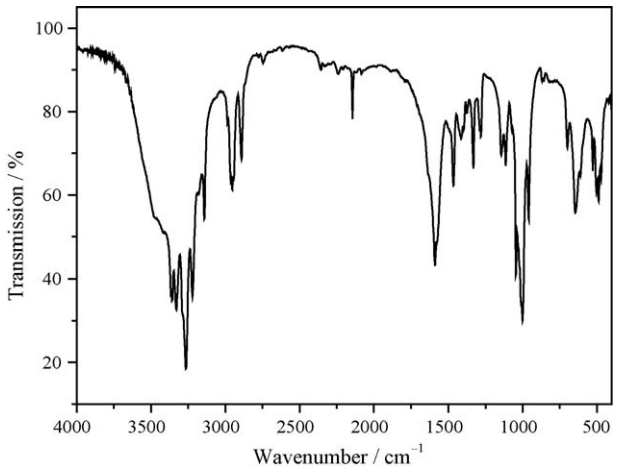


Fig. 2. Infrared spectrum of tris(ethylenediamine)zinc tetracyanozincate.

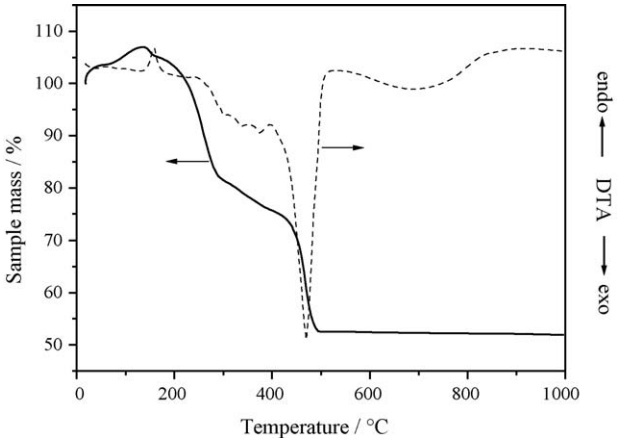


Fig. 3. Thermogravimetry of tris(ethylenediamine)zinc tetracyanozincate under dynamic oxygen atmosphere.

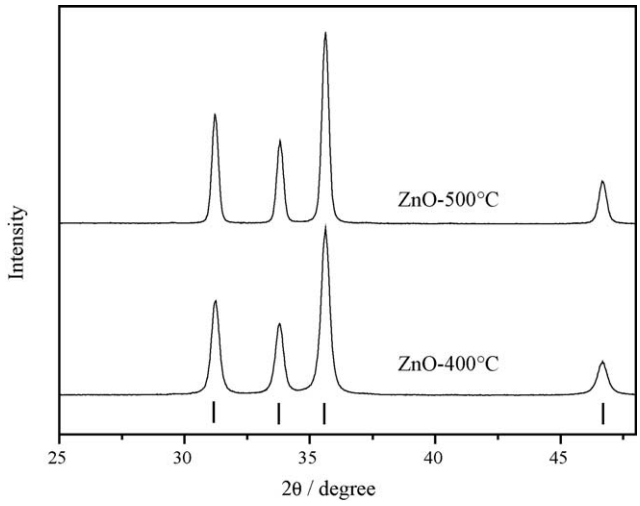


Fig. 4. X-ray diffraction patterns of the thermolysis products of tris(ethylenediamine)zinc tetracyanozincate: ZnO, obtained at 400 and 500 °C under air. The data were converted to Cu Kα radiation (λ = 1.54 Å).

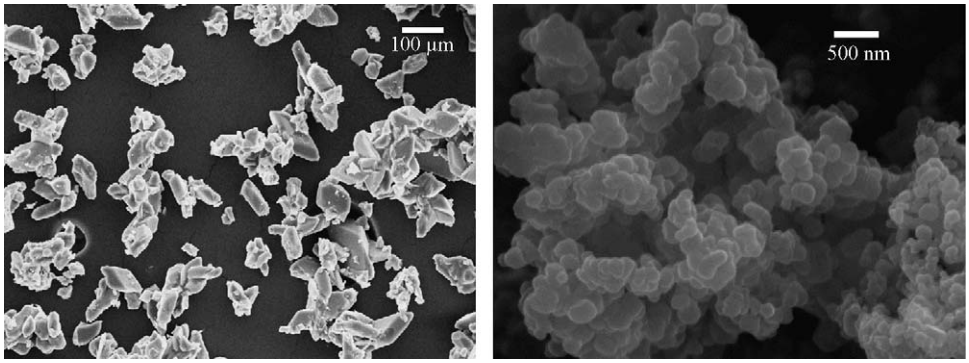


Fig. 5. Scanning electron micrographs of crystals of the precursor tris(ethylenediamine)zinc tetracyanozincate, and of the reaction product ZnO after thermolysis at 500 °C.

the ethylenediamine is released without combustion in an endothermic process around 150 °C. Above about 200 °C this is followed by the exothermic decomposition (combustion) of the remaining ethylenediamine and the cyanide which ceases close to 500 °C. The observed total mass loss of 55.1 wt% (using the maximum weight as reference) was smaller than the expected value of 60.7 wt% for the reaction product ZnO. Because the residue after thermogravimetry was clearly identified as pure ZnO by X-ray diffraction (see also below) and crystalline side products can be ruled out, a possible explanation could be a deviation of the stoichiometry of the initial zinc complex from its ideal formula, e.g., it might have contained less than three ethylenediamine ligands (note that the thermobalance was evacuated before the experiment, i.e., before flooding it with oxygen).

It was reported earlier that ethylenediamine was the first leaving group during the thermal decomposition of $[Zn(en)_3][Ni(CN)_4]$ [26]. In our case, a weight loss of 37.6 wt% was observed up to the step in the TG curve at 430 °C, being close to an expected weight loss of 43.4 wt% from $[Zn(en)_3][Zn(CN)_4]$ to $Zn[Zn(CN)_4] = Zn(CN)_2$. This suggests that the leaving of ethylenediamine dominates the first step of decomposition, in agreement with the literature.

When heated in a furnace under air at 400 or 500 °C for 3 h, the precursor fully decomposed to zinc oxide. Note that this temperature is the lowest which was possible for complete decomposition, and that it was chosen to avoid thermal sintering of the formed ZnO. This is shown by X-ray diffraction data (Fig. 4). No other crystalline phases were found.

Zinc oxide was obtained in the form of nanoparticles with a typical particle size of 200 nm, with no difference between a thermolysis at 400 or 500 °C (Fig. 5). The rhombohedral morphology of the precursor compound was fully destroyed during thermolysis, i.e., no topotactic or topochemical reaction [27] occurred.

## 4. Conclusions

The binuclear complex $[Zn(en)_3][Zn(CN)_4]$ was prepared and the crystal structure of this compound was determined for the first time. Under oxygen, the thermolysis of the complex $[Zn(en)_3][Zn(CN)_4]$ leads to ZnO nanoparticles with a size of 100–300 nm. There is no correlation between the morphology of the crystals of the parent compound and the ZnO crystals, i.e., the structure completely breaks down during thermolysis. It was found that the decomposition of the cyanide compound under oxygen occurred in multi-steps in the range of 150–500 °C. The thermolysis of this Zn-based coordination compounds is a useful synthetic route to nanosized ZnO.

## Acknowledgments

We thank the Deutsche Forschungsgemeinschaft (SFB 558: metal–substrate interactions in heterogeneous catalysis) for financial support. Synchrotron beamtime by HASYLAB at DESY was generously provided.

## References

[1] N. Uekawa, R. Yamashita, Y. Wu, K. Kakegawa, Phys. Chem. Chem. Phys. 6 (2004) 442.
[2] M. Mo, J.C. Yu, L. Zhang, S.A. Li, Adv. Mater. 17 (2005) 756.
[3] J.Y. Lao, J.G. Wen, Z.F. Ren, Nano Lett. 2 (2002) 1287.
[4] K.S. Choi, H.C. Lichtenegger, G.D. Stucky, E.W. McFarland, J. Am. Chem. Soc. 124 (2002) 12402.
[5] P.X. Gao, Z.L. Wang, J. Am. Chem. Soc. 125 (2003) 11299.
[6] H. Wilmer, M. Kurtz, K. Klementiev, O. Tkachenko, W. Grünert, O. Hinrichsen, A. Birkner, S. Rabe, K. Merz, M. Driess, C. Wöll, M. Muhler, Phys. Chem. Chem. Phys. 5 (2003) 4736.
[7] L. Vayssieres, Adv. Mater. 15 (2003) 464.
[8] J.Q. Hu, Y. Bando, J.H. Zhan, Y.B. Li, T. Sekiguchi, Appl. Phys. Lett. 83 (2003) 4414.
[9] J.Q. Hu, Q. Li, X.M. Meng, C.S. Lee, S.T. Lee, Chem. Mater. 15 (2003) 305.
[10] F. Li, Y. Ding, P. Gao, X. Xin, Z.L. Wang, Angew. Chem. Int. Ed. 43 (2004) 5238.
[11] W.I. Park, G.C. Yi, Adv. Mater. 16 (2004) 87.
[12] X.Y. Kong, Y. Ding, R. Yang, Z.L. Wang, Science 303 (2004) 1348.
[13] Z.K. Tang, G.K.L. Wong, P. Yu, M. Kawasaki, A. Ohtomo, H. Koinuma, Y. Segawa, Appl. Phys. Lett. 72 (1998) 3270.
[14] C. Pacholski, A. Kornowski, H. Weller, Angew. Chem. Int. Ed. 41 (2002) 1188.
[15] M. Shim, P. Guyot-Sionnest, J. Am. Chem. Soc. 123 (2001) 11651.
[16] J. Hambrock, S.M. Rabe, K.A. Birkner, A. Wohlfart, R.A. Fischer, M. Driess, J. Mater. Chem. 13 (2003) 1731.
[17] M. Rehbein, M. Epple, R.D. Fischer, Solid State Sci. 2 (2000) 473.
[18] M. Rehbein, R.D. Fischer, M. Epple, Thermochim. Acta 382 (2002) 143.
[19] Y. Guo, R. Weiss, M. Epple, J. Mater. Chem. 15 (2005) 424.

[20] Y. Guo, R. Weiss, M. Epple, Eur. J. Inorg. Chem. (2005) 3072.
[21] R. Weiss, G. Jansen, R. Boese, M. Epple, Dalton Trans., in press.
[22] J. Cernak, J. Chomic, C. Kappenstein, M. Dunaj-Jurco, Z. Kristallogr. 209 (1994) 430.
[23] D. Neill, M.J. Riley, C.H.L. Kennard, Acta Crystallogr. C 53 (1997) 701.
[24] C. Wieczorrek, Acta Crystallogr. C 56 (2000) 1079.
[25] D.X. Jia, Y. Zhang, J. Dai, Q.Y. Zhu, X.M. Gu, Z. Anorg. Allg. Chem. 630 (2004) 313.
[26] J. Cernak, I. Potocnak, J. Chomic, J. Therm. Anal. Cal. 39 (1993) 849.
[27] G.M.J. Schmidt, M.D. Cohen, J. Chem. Soc. (1964) 01996.